

Computational and Numerical Properties of a Broadband Subspace-Based Likelihood Ratio Test

Cornelius A.D. Pahalson, Louise H. Crockett, and Stephan Weiss

Department of Electronic & Electrical Engineering, University of Strathclyde, Glasgow, Scotland
 {cornelius.pahalson,louise.crockett,stephan.weiss}@strath.ac.uk

Abstract—This paper investigates the performance of a likelihood ratio test in combination with a polynomial subspace projection approach to detect weak transient signals in broadband array data. Based on previous empirical evidence that a likelihood ratio test is advantageously applied in a lower-dimensional subspace, we present analysis that highlights how the polynomial subspace projection whitens a crucial part of the signals, enabling a detector to operate with a shortened temporal window. This reduction in temporal correlation, together with a spatial compaction of the data, also leads to both computational and numerical advantages over a likelihood ratio test that is directly applied to the array data. The results of our analysis are illustrated by examples and simulations.

I. INTRODUCTION

A number of applications require the detection of weak transient broadband signals in the presence of more dominant signals or interference. This includes, for example, the task of detecting an emerging primary user in a cognitive radio environment [1]–[7], of condition monitoring and testing for electromagnetic compatibility [8], or for registering seismic events [9]. In a defence context, it is often desirable if not vital to detect a weak transient source in underwater/sonar [10] or radio frequency domain scenarios [11]. Similarly, there may be a need to detect the presence of a new speaker in an audio environment against several stronger, overlapping speakers [12] or against general background noise [13].

The detection of transient signals can rely on energy-based criteria and utilise short-time Fourier transform-type or wavelet-based approaches to identify the correlation structure that transients may be expected to possess [14]–[16]. Data-dependent transforms, for example the Karhunen-Loeve transform [17], reached via an eigenvalue decomposition (EVD) of the data covariance matrix, can attain optimality in terms of energy compaction into a lower-dimensional subspace. Related subspace partitioning approaches have been used in e.g. [18]–[22]. More recently, machine learning methods have also been attempted [10], [23], but require a sufficient amount of data in order to be trained off-line.

In order to address the problem of broadband transient signal detection within a reasonable computational error, in the past we have suggested a broadband or polynomial subspace approach [11]. It is based on the assumption that L sources that are stationary for a sufficient amount of time illuminate M sensors, with $M > L$. The propagation environment is

broadband, such that the sources arrive convolutively mixed, i.e. possess both temporal and spatial correlation. In the presence of these signals, we would like to detect the presence of a transient signal. This scenario is outlined in Fig. 1; all signal sources are assumed to be Gaussian, and we are only given the measurements $\mathbf{x}[n]$ but are blind to the source model, with the convolutive mixing systems that generate those measurements.

The statistically optimum test, the likelihood ratio test (LRT), in the case of Gaussian data is based on the covariance of the data with and without the transient signal [5], [24], [25]. For broadband signals, temporal averaging in the LRT needs to take the temporal correlation of the signals into account — this leads to potentially large space-time covariance matrices that require inversion [7]. For this reason, in [7], the LRT has been combined with a relatively inexpensive subspace approach, where the LRT is applied to a lower-dimensional subspace projection rather than to the original data. This was motivated by the fact that the subspace method itself — known for the narrowband case in [18]–[22] — was successfully deployed for weak transient signal detection [11]–[13].

For the weak transient signal detection in [11]–[13], it is assumed that over a past period of time, the statistics of the stationary signals can be estimated. Going forward in time, a change point detection would aim to find any change in the signal energy. This change point detection has been easier to apply to a lower-dimensional vector $\mathbf{s}[n]$, which is a projection onto the noise-only subspace of the covariance matrix based on the stationary sources, than on the measurements $\mathbf{x}[n]$ [11]. For this approach, the particular statistics of the transient source were not required to be known. However, in order to assess how close this approach was to an optimal detection method, we applied an LRT and a generalised LRT to both the

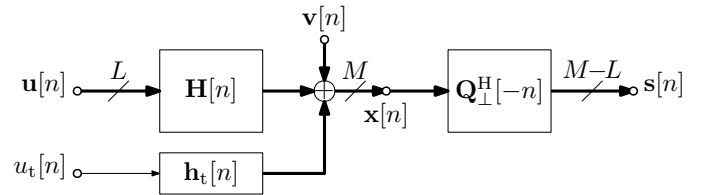


Fig. 1. Signal model with measurement $\mathbf{x}[n] \in \mathbb{C}^M$, containing stationary sources $\mathbf{u}[n] \in \mathbb{C}^L$ and a transient source $u_t[n]$, and processing by $\mathbf{G}[n]$ to yield a subspace projection $\mathbf{y}[n] \in \mathbb{C}^{M-L}$.

Cornelius Pahalson acknowledges support by the Tertiary Education Trust Fund, Nigeria.

measurements and the projected data in [7], with significant empirical benefits for the later.

Therefore, the aim of this paper is to explore why the polynomial subspace approach is so beneficial for a combination with the LRT. Particularly two issues have been noted in [7] with respect to the temporal window T , i.e. basing a decision not just on a single snap-shot but a sequence of T time instances:

- 1) for small T , the subspace-based approach outperforms an LRT applied directly to the measurements;
- 2) for larger T , applying the LRT to the data rather than the projection can result in severe numerical problems.

The contribution of this paper is to provide the theoretical foundation to understand both points.

Below, the system model, as well as the broadband subspace decomposition and projection are outlined in Sec. II. Sec. III reviews the LRT method. The main contribution of this paper is Sec. IV, which analyses the LRT when applied to both measurement and projected data, followed by examples and simulations in Sec. V.

II. SPACE-TIME COVARIANCE AND POLYNOMIAL SUBSPACE APPROACH

A. Signal Model and Space-Time Covariance

To expand on the signal model of Sec. I in Fig. 1, we assume that in the stationary case, contributions by L sources are received by $M > L$ sensors via a convolutive mixing matrix $\mathbf{H}[n] \in \mathbb{C}^{M \times L}$. The sources, gathered in a signal vector $\mathbf{u}[n] \in \mathbb{C}^L$, are mutually independent, temporally uncorrelated, with zero mean and unit variance signals $u_\ell[n]$, $\ell = 1, \dots, L$, such that $\mathbf{u}[n] = [u_1[n], \dots, u_L[n]]^T \sim \mathcal{CN}(\mathbf{0}, \mathbf{I}_L)$. Any specific source power spectral densities are captured in the model of Fig. 1 via the convolutive mixing matrix $\mathbf{H}[n]$, which also operates as an innovation filter [26]. The data received from the sources is corrupted by additive complex Gaussian noise $\mathbf{v}[n] \sim \mathcal{CN}(\mathbf{0}, \sigma_v^2 \mathbf{I}_M)$. A transient signal potentially illuminates the array via a vector of filters $\mathbf{h}_t[n] \in \mathbb{C}^M$ to another uncorrelated signal $u_{L+1}[n] \sim \mathcal{CN}(0, \sigma_t^2)$, whose presence we would like to detect.

For the space-time covariance, based on the expectation $\mathcal{E}\{\cdot\}$ and Hermitian transpose operator $\{\cdot\}^H$, we have $\mathbf{R}[\tau] = \mathcal{E}\{\mathbf{x}[n]\mathbf{x}^H[n+\tau]\}$ of the measurement vector $\mathbf{x}[n]$. We first consider the absence of the transient signal, i.e. $u_{L+1}[n] = 0$. In this case, for the cross-spectral density (CSD) $\mathbf{R}(z) = \sum_\tau \mathbf{R}[\tau]z^{-\tau}$, or short $\mathbf{R}[\tau] \circ \bullet \mathbf{R}(z)$, we obtain

$$\mathbf{R}(z) = \mathbf{H}(z)\mathbf{H}^P(z) + \sigma_v^2 \mathbf{I}_M. \quad (1)$$

In (1), $\mathbf{H}(z) \bullet \mathbf{H}[n]$ represents a matrix of transfer functions. The parahermitian operator $\{\cdot\}^P$ implies a Hermitian transposition and time reversal, such that $\mathbf{H}^P(z) = \{\mathbf{H}(1/z^*)\}^H$ [27]. Hence, $\mathbf{R}(z)$ is a parahermitian matrix that satisfies $\mathbf{R}^P(z) = \mathbf{R}(z)$.

If $u_{L+1}[n] \neq 0$, then this signal's contribution to the overall CSD matrix is

$$\mathbf{R}_t(z) = \mathbf{h}_t(z)\mathbf{h}_t^P(z), \quad (2)$$

with $\mathbf{h}_t(z) \bullet \mathbf{h}[n]$. The overall CSD of the measurement vector $\mathbf{x}[n]$ thus is $\mathbf{R}(z) + \mathbf{R}_t(z)$, whereby $\mathbf{R}_t(z)$ is a rank one contribution.

B. Analytic Eigenvalue Decomposition

Given the signal model in Fig. 1, the CSD matrix $\mathbf{R}(z)$ is analytic in z and admits an analytic EVD [28]–[31]

$$\mathbf{R}(z) = \mathbf{Q}(z)\mathbf{\Lambda}(z)\mathbf{Q}^P(z). \quad (3)$$

In (3), $\mathbf{\Lambda}(z) = \text{diag}\{\lambda_1(z), \dots, \lambda_M(z)\}$ is a diagonal parahermitian matrix holding the analytic eigenvalues $\lambda_m(z)$, $m = 1, \dots, M$ of $\mathbf{R}(z)$. Their corresponding eigenvectors form the columns of $\mathbf{Q}(z)$, which is also analytic in z and satisfies paraunitarity, such that $\mathbf{Q}^P(z)\mathbf{Q}(z) = \mathbf{Q}(z)\mathbf{Q}^P(z) = \mathbf{I}_M$, and therefore $\mathbf{Q}^{-1}(z) = \mathbf{Q}(z)$ result [27]. Analyticity of the factors in (3) is important, as this property permits to approximate $\mathbf{Q}(z)$ arbitrarily closely by polynomials of sufficient order by shift and truncation operations [32]–[34].

Based on (3), we can define subspace decomposition,

$$\mathbf{\Lambda}(z) = \begin{bmatrix} \mathbf{\Lambda}_H(z) + \sigma_v^2 \mathbf{I}_L & \\ & \sigma_v^2 \mathbf{I}_{M-L} \end{bmatrix}, \quad (4)$$

$$\mathbf{Q}(z) = [\mathbf{Q}_\parallel(z), \mathbf{Q}_\perp(z)], \quad (5)$$

where $\mathbf{\Lambda}_H(z)$ holds the L analytic eigenvalues of $\mathbf{H}(z)\mathbf{H}^P(z) : \mathbb{C} \rightarrow \mathbb{C}^{L \times L}$, and $\mathbf{Q}_\parallel(z)$ contains their corresponding eigenvectors. The orthogonal complement $\mathbf{Q}_\perp(z)$, such that $\mathbf{Q}_\perp^P(z)\mathbf{Q}_\parallel(z) = \mathbf{0}$, contains analytic eigenvectors that span the noise-only subspace of $\mathbf{R}(z)$. This noise-only subspace does not contain any contributions by the L stationary sources.

In practice, analytic EVD algorithms [32], [35]–[40] operate in the DFT domain. In case the eigenvalues are spectrally majorised, e.g. because of estimation [41]–[44], polynomial EVD algorithms [45]–[52] can yield similar results. Computationally efficient implementations of such decompositions have been considered in e.g. [53], [54]; the order of $\mathbf{Q}(z)$ — which will determine the order and therefore computational cost of filters in applications — can be reduced through limiting its order through shifts and truncations [32]–[34], [55], [56].

C. Subspace Projection

With the partitioning of the analytic SVD factors in (4) and (5), $\mathbf{Q}_\perp(z) \bullet \mathbf{Q}_\perp[n]$ can be used to project the measurement data $\mathbf{x}[n]$ into the noise-only subspace,

$$\mathbf{s}[n] = \sum_\nu \mathbf{Q}_\perp^H[-\nu]\mathbf{x}[n-\nu], \quad (6)$$

where $\mathbf{s}[n] \in \mathbb{C}^{M-L}$ is the projected data, as shown in Fig. 1. In the ideal case, this new signal vector $\mathbf{s}[n]$ is now free of any contributions from the L stationary sources. In contrast, with the emergence of the transient signal $u_{L+1}[n]$, there are now $L+1$ signals in the environment, and at least some part of $u_{L+1}[n]$ will project into $\mathbf{s}[n]$, where its presence can be more easily detected than in the measurements $\mathbf{x}[n]$.

Because part of the broadband signal $u_{L+1}[n]$ is projected into the noise-only subspace vector $\mathbf{s}[n]$, the latter has also

been termed a syndrome vector in [11]. This terminology is borrowed from coding theory and in particular from filter-bank based source-channel coding methods [57], where a broadband subspace that is orthogonal to the code subspace is indicative of impulse noise and other transmission errors. The operation in (6) represents a generalisation of narrowband subspace detection approaches [18]; the extension to the broadband case via (6) has been utilised for voice activity detection in the presence of stronger speakers [12] or noise [13]. Such polynomial subspace decompositions have also been applied, for example, in the context of joint source-channel coding [58], angle of arrival estimation [59]–[61], source separation [62] and localisation [63], beamforming [64], [65], and channel identification [66].

III. LIKELIHOOD RATIO TEST

We now follow the approach in [7], where a likelihood ratio approach can be applied to either the measurement data $\mathbf{x}[n]$ or to its subspace projection $\mathbf{s}[n]$. We first briefly comment on the LRT formulation before we focus on the two application cases.

A. Likelihood Ratio Test

For a general exploration of the likelihood ratio test, we utilise a test variable $\mathbf{y}_n \in \mathbb{C}^K$, which can later be constructed from measurement vectors $\mathbf{x}[n]$ or syndrome vectors $\mathbf{s}[n]$, including a concatenation of temporal snapshots. The dimension K will therefore depend on this choice. We assume that \mathbf{y}_n can consist of $\mathbf{y}_{0,n} \in \mathbb{C}^K$, which is the stationary noise, and $\mathbf{y}_{1,n} \in \mathbb{C}^K$, representing the transient component. Both signals are assumed to be zero mean complex Gaussian with $\mathbf{y}_{0,n} \sim \mathcal{CN}(\mathbf{0}, \mathbf{R}_0)$ and $\mathbf{y}_{1,n} \sim \mathcal{CN}(\mathbf{0}, \mathbf{R}_1)$. The aim is thus to distinguish between the two hypotheses

$$\begin{aligned} H_0 : \quad \mathbf{y}_n &= \mathbf{y}_{0,n} , \\ H_1 : \quad \mathbf{y}_n &= \mathbf{y}_{0,n} + \mathbf{y}_{1,n} . \end{aligned}$$

In our context, $\mathbf{y}_{0,n}$ holds the contribution from the L stationary sources and additive noise, while $\mathbf{y}_{1,n}$ comprises of components due to the transient signal. The probability density functions for \mathbf{y}_n , under the two hypotheses are then given by

$$p(\mathbf{y}_n|H_0) = (2\pi|\mathbf{R}_0|)^{-\frac{1}{2}} e^{-\frac{1}{2}\mathbf{y}_n^H \mathbf{R}_0^{-1} \mathbf{y}_n} , \quad (7)$$

$$p(\mathbf{y}_n|H_1) = (2\pi|\mathbf{R}_0 + \mathbf{R}_1|)^{-\frac{1}{2}} e^{-\frac{1}{2}\mathbf{y}_n^H (\mathbf{R}_0 + \mathbf{R}_1)^{-1} \mathbf{y}_n} , \quad (8)$$

where the determinant of a matrix \mathbf{X} is denoted as $|\mathbf{X}|$.

For the likelihood ratio $L(\mathbf{y}_n)$, we have

$$L(\mathbf{y}_n) = \frac{p(\mathbf{y}_n|H_0)}{p(\mathbf{y}_n|H_1)} = \frac{|\mathbf{R}_0 + \mathbf{R}_1|^{\frac{1}{2}}}{|\mathbf{R}_0|^{\frac{1}{2}}} e^{-\frac{1}{2}\mathbf{y}_n^H \mathbf{A} \mathbf{y}_n} , \quad (9)$$

where for brevity

$$\mathbf{A} = \mathbf{R}_0^{-1} - (\mathbf{R}_0 + \mathbf{R}_1)^{-1} . \quad (10)$$

With its EVD $\mathbf{A} = \mathbf{Q}\mathbf{\Lambda}\mathbf{Q}^H$, the likelihood ratio can be further expressed as

$$L(\mathbf{y}_n) = \frac{|\mathbf{R}_0 + \mathbf{R}_1|^{\frac{1}{2}}}{|\mathbf{R}_0|^{\frac{1}{2}}} e^{-\frac{1}{2}\|\mathbf{\Lambda}^{\frac{1}{2}}\mathbf{Q}^H \mathbf{y}_n\|_2^2} . \quad (11)$$

In order to accept or reject the hypothesis, we now need to find a threshold c such that

$$L(\mathbf{y}_n) \underset{H_1}{\overset{H_0}{\gtrless}} c . \quad (12)$$

Rearranging leads to

$$\|\mathbf{\Lambda}^{\frac{1}{2}}\mathbf{Q}^H \mathbf{y}_n\| \underset{H_1}{\overset{H_0}{\gtrless}} 2 \ln \left\{ \frac{|\mathbf{R}_0|^{\frac{1}{2}}}{|\mathbf{R}_0 + \mathbf{R}_1|^{\frac{1}{2}}} c \right\} = c' , \quad (13)$$

where c' is a modified threshold. With the term $\|\mathbf{\Lambda}^{\frac{1}{2}}\mathbf{Q}^H \mathbf{y}_n\|$, we have defined the test statistic for the likelihood ratio test.

B. Likelihood Ratio Test on Measurements

Applying the LRT directly to the measurement data in principle exploits all information that we can possibly draw from it. For the purpose of temporal averaging the test outcome, for the LRT variable \mathbf{y}_n we utilise a concatenation of T snapshots of $\mathbf{x}[n]$,

$$\mathbf{y}_n^H = [\mathbf{x}_n^H, \mathbf{x}_{n-1}^H, \dots, \mathbf{x}_{n-T+1}^H] , \quad (14)$$

such that $\mathbf{y}_n \in \mathbb{C}^{MT}$.

For the covariance matrices in (10), we introduce extra subscripts to denote their reference to the measurement vector via $\mathbf{R}_{\mathbf{x},0}$ and $\mathbf{R}_{\mathbf{x},1}$. For the covariance covering the hypothesis H_0 , we have

$$\mathbf{R}_{\mathbf{x},0} = \begin{bmatrix} \mathbf{R}[0] & \dots & \mathbf{R}[T-1] \\ \vdots & \ddots & \vdots \\ \mathbf{R}[1-T] & \dots & \mathbf{R}[0] \end{bmatrix} , \quad (15)$$

where (1) defines $\mathbf{R}[\tau] \circ \bullet \mathbf{R}(z)$. Similarly, $\mathbf{R}_{\mathbf{x},1}$ can be constructed from the lag components of $\mathbf{R}_t[\tau]$ in (2). Both covariance matrices $\mathbf{R}_{\mathbf{x},i}$, $i = 0, 1$, are of dimension $(MT) \times (MT)$. Thus the inversions required for (10) can present computational and numerical challenges, which we will address separately in Sec. IV.

C. Likelihood Ratio Test on Subspace Data

In order to apply the likelihood ratio test to T successive samples of the projected data vector $\mathbf{s}[n]$, we define analogously to (14) the variable

$$\mathbf{y}_n^H = [\mathbf{s}_n^H, \mathbf{s}_{n-1}^H, \dots, \mathbf{s}_{n-T+1}^H] , \quad (16)$$

where now $\mathbf{y}_n \in \mathbb{C}^{(M-L)T}$. For its space-time covariance $\mathbf{R}'[\tau] = \mathcal{E}\{\mathbf{y}[n]\mathbf{y}^H[n-\tau]\}$ and the corresponding CSD matrix $\mathbf{R}'(z) : \mathbb{C} \rightarrow \mathbb{C}^{(M-L) \times (M-L)}$, we can state

$$\mathbf{R}'(z) = \mathbf{Q}'_{\perp}(z)\mathbf{R}(z)\mathbf{Q}'_{\perp}(z) , \quad (17)$$

with respect to the CSD matrix of the measurement data, $\mathbf{R}(z)$, in Sec. III-B. Analogous to (III-B), we can now obtain $\mathbf{R}_{\mathbf{s},0}$ from the matrix-valued coefficients of $\mathbf{R}'[n] \circ \bullet \mathbf{R}'(z)$.

For the transient component, we can define

$$\mathbf{R}'_t(z) = \mathbf{Q}'_{\perp}(z)\mathbf{R}_t(z)\mathbf{Q}'_{\perp}(z) , \quad (18)$$

based on the rank-one term $\mathbf{R}_t(z)$ in (2). Analogously to (III-B), we can obtain a constant covariance matrix $\mathbf{R}_{\mathbf{s},0}$

from $\mathbf{R}'_t[n] \circ \rightarrow \mathbf{R}'_t(z)$. Overall, in the subspace-based case we now have covariance matrices $\mathbf{R}_{s,i}$, $i = 0, 1$, of size $T(M-L) \times T(M-L)$.

D. Application and Generalised LRT

The application of the above LRT test to data typically assumes that the covariance matrices under the two hypothesis are known — \mathbf{R}_0 for H_0 , and the composite $(\mathbf{R}_0 + \mathbf{R}_1)$ for H_1 — independent of whether these are derived from the measurements or the subspace-projected data. The covariance matrices represent the exact ensemble statistics, i.e. the source model of Fig. 1 is known a priori. In practise, where only finite data is available to estimate the statistics, an estimated space-time covariance $\hat{\mathbf{R}}(z)$ will be subject to estimation errors that depend on both the sample size of the data, as well as on the ground truth $\mathbf{R}(z)$ [41]–[44], thus resulting in estimates $\hat{\mathbf{R}}_0$ and $(\hat{\mathbf{R}}_0 + \hat{\mathbf{R}}_1)$. This reliance on potentially inaccurate estimates turns the LRT into a generalised likelihood ratio test (GLRT).

Recall that the aim of this paper is to explore the optimality of the test. For our application outlined in Sec. I, we have an estimate $\hat{\mathbf{R}}_0$, but we are not able to measure $\hat{\mathbf{R}}_1$, neither by itself or in combination with $\hat{\mathbf{R}}_0$, ahead of performing a change point detection. Knowing what is optimally achievable given either \mathbf{R}_i or $\hat{\mathbf{R}}_i$ provide a useful benchmark for [11] and applications such as [12], [13].

IV. ANALYSIS OF SUBSPACE-BASED LRT

In this section we explore properties of the covariance matrices $\mathbf{R}_{x,i}$, $i = 0, 1$, for the measurements and of $\mathbf{R}_{s,i}$, $i = 0, 1$, for the projected data, that feed into the LRT discussed in Sec. III.

A. Consideration of Temporal Correlation

We first focus on the hypothesis H_0 , where only L stationary signals are present. In this case, if the mixing system $\mathbf{H}(z)$ consists of FIR filters of length $(J+1)$, i.e. it is a polynomial matrix of order J , then $\mathbf{R}(z)$ is a Laurent polynomial matrix of order $2J$. Generally, this matrix will be dense in the sense that generally all its coefficients $\mathbf{R}[\tau]$ for $|\tau| \leq J$ will have non-zero elements. As a result, for the consideration of a temporal window $T < J$ in the LRT, $\mathbf{R}_{x,0}$ will be a dense matrix. Only for the case $T > J$ will we start to see zero corner blocks to appear.

Inspecting the projected data under hypothesis H_0 , we have $\mathbf{R}'(z)$ given by (17). With the subspace partitioning in (4) and (5), this simplifies in the case of an ideal EVD to

$$\mathbf{R}'(z) = \sigma_v^2 \mathbf{I}_{M-L}, \quad (19)$$

since the projection we have orthogonality of the signal subspace, i.e. $\mathbf{Q}_{\perp}^P(z)\mathbf{H}(z) = \mathbf{0}$. Thus, for the LRT test we obtain

$$\mathbf{R}_{s,0} = \sigma_v^2 \mathbf{I}_{(M-L)T}. \quad (20)$$

In contrast to $\mathbf{R}_{x,0}$ for the measurement data, (20) shows that under H_0 , the test variable \mathbf{y}_n in (16) is spatially and

temporally uncorrelated. Typically temporal correlation will degrade a test variable [11] which is avoided for the projected data under H_0 .

Under hypothesis H_1 , we have the covariance matrix $(\mathbf{R}_0 + \mathbf{R}_1)$. For both the measurement case and the projected data case, $\mathbf{R}_{x,1}$ and $\mathbf{R}_{s,1}$ will now be dense matrices, and the input data to the LRT, \mathbf{y}_n , in both cases will be temporally and spatially correlated. Due to passing through the filter bank $\mathbf{Q}_{\perp}^P(z)$, the projected data will be correlated over an even longer data window compared to the measurement data.

To build the matrix \mathbf{A} in (10) for the LRT, consider that both $\mathbf{R}_t(z)$ and $\mathbf{R}'_t(z)$ are rank one matrices as evident from the outer products in (2) and (18), whereby for the latter we can define $\mathbf{R}'_t(z) = \mathbf{Q}_{\perp}^P(z)\mathbf{h}_t(z)\mathbf{h}_t^P(z)\mathbf{Q}_{\perp}^P(z) = \mathbf{h}'_t(z)\mathbf{h}'_t^P(z)$ with the $\mathbf{h}'_t(z) = \mathbf{Q}_{\perp}^P(z)\mathbf{h}_t(z) : \mathbb{C} \rightarrow \mathbb{C}^{M-L}$ a vector of functions. As a result of the space-time covariance having rank one, at least theoretically the covariance matrices $\mathbf{R}_{x,1}$ and $\mathbf{R}_{s,0}$ will have at most rank T [65] and can be factorised as

$$\mathbf{R}_{x,1} = \mathbf{H}_t \mathbf{H}_t^H \quad (21)$$

$$\mathbf{R}_{s,1} = \mathbf{H}'_t \mathbf{H}'_t^H \quad (22)$$

where $\mathbf{H}_t \in \mathbb{C}^{MT \times T}$ and $\mathbf{H}'_t \in \mathbb{C}^{(M-L)T \times T}$.

Using the Woodbury identity for the low-rank update $(\mathbf{R}_0 + \mathbf{R}_1)^{-1}$, for (10) we obtain in general

$$\mathbf{A} = \mathbf{R}_0^{-1} \mathbf{H}_t (\mathbf{I}_T + \mathbf{H}_t^H \mathbf{R}_0^{-1} \mathbf{H}_t)^{-1} \mathbf{H}_t^H \mathbf{R}_0^{-1}. \quad (23)$$

When (23) specifically for the measurement case, then the dense nature of $\mathbf{R}_{x,0}$ does not allow for further simplifications. In the case of the projected data, here referred to as \mathbf{A}_s , we have

$$\mathbf{A}_s = \frac{1}{\sigma_v^2} \mathbf{H}'_t (\sigma_v^2 \mathbf{I}_T + \mathbf{H}'_t^H \mathbf{H}'_t)^{-1} \mathbf{H}'_t^H. \quad (24)$$

Although (23) and (24) do not represent how the processor for the test statistic in (13) is computed since only \mathbf{R}_0 and $(\mathbf{R}_0 + \mathbf{R}_1)$ are available, (24) provides some insight into how the projected data case simplifies the underlying procedure — it provides an outer product between a low rank matrix \mathbf{H}'_t and its regularised left pseudo-inverse, that is free of any temporal or spatial correlations imposed by the stationary sources captured in \mathbf{R}_0 .

B. Consideration of Covariance Matrix Conditioning

We now want to assess how the computation of the inverses for \mathbf{R}_0 and $(\mathbf{R}_0 + \mathbf{R}_1)$ are affected by whether we operate the LRT on the measurements or the projected data. We assess this via the condition number of a matrix [67], which assesses the gain w.r.t. any random perturbations — e.g. through estimation errors [42] — in the inversion process.

For the measurement case, the condition number of $\mathbf{R}_{x,0}$ can be related to the eigenvalue spread [17] of the signals, which assesses the ratio between the minimum and maximum

spectral value and here additionally has a spatial component. For the maximum eigenvalue, we have

$$\max\{\lambda_{x,0}\} = \max_{\Omega,m} \lambda\{\mathbf{R}(e^{j\Omega})\} \quad (25)$$

$$\approx \max_{\Omega,m} \lambda\{\mathbf{H}(e^{j\Omega})\mathbf{H}^P(e^{j\Omega})\} > \sigma_s^2, \quad (26)$$

where $\lambda\{\mathbf{R}(z)\}$ returns the analytic eigenvalues of the para-hermitian matrix $\mathbf{R}(z)$ [28], and σ_s^2 is the maximum power of a stationary source in a measurement $x_m[n]$, assuming for the SNR $\sigma_s^2/\sigma_v^2 \gg 1$. For the smallest eigenvalue, the noise floor in the noise-only subspace will be given by σ_v^2 , such that we obtain

$$\gamma_{x,0} > \sigma_s^2/\sigma_v^2 \quad (27)$$

for the condition number under H_0 . Under H_1 , the maximum eigenvalue is still due to a strong stationary component, while the minimum possible eigenvalue remains given by the noise floor. Hence, we have approximately $\gamma_{x,1} = \gamma_{x,0}$.

For the case of projected data, ideally the stationary signals are no longer present. In this case, the maximum eigenvalue is given by the

$$\max\{\lambda_{s,0}\} = \max_{\Omega,m} \lambda\{\mathbf{R}'(e^{j\Omega})\} \quad (28)$$

$$\begin{aligned} &= \max_{\Omega,m} \lambda\{\mathbf{H}_t(e^{j\Omega})\mathbf{H}_t^P(e^{j\Omega}) + \sigma_v^2\mathbf{I}_{T(M-L)}\} \\ &> \sigma_t^2 + \sigma_v^2, \end{aligned} \quad (29)$$

where σ_t^2 represents the maximum power of the transient signal in any of the measurement signals $x_m[n]$. Note that this power is not increased when passing through $\mathbf{Q}^P(z)$, since this matrix completes to a paraunitary and therefore energy-preserving system. Since the smallest eigenvalue is still limited by the noise floor, we therefore have $\gamma_{s,0} > 1$ and

$$\gamma_{s,1} > \frac{\sigma_t^2 + \sigma_v^2}{\sigma_v^2} \quad (30)$$

for the condition number under hypotheses H_0 and H_1 . Note that in the case that the transient signal is significantly weaker than the stationary signals, the covariance matrices for the projected data have a much lower bound for the condition number and generally will be much better conditioned than their equivalent quantities based on the measurement data.

V. SIMULATIONS AND RESULTS

A. System Setup and Performance Metrics

To demonstrate the LRT and its analysis, with reference to Fig. 1 we investigate a scenario where we have $M = 10$ sensors picking up signals from $L = 7$ independent stationary sources via a mixing system $\mathbf{H}(z)$ of two different orders $J = \{10; 20\}$. The SNR of these signal is 20 dB w.r.t. additive complex-valued uncorrelated Gaussian noise of variance σ_v^2 . A transient source is undergoing a source model of the same order as $\mathbf{R}(z)$ and at the sensors possess as powers that are $\{10; 20\}$ dB below the stationary signals, i.e. in the second setting the transient signal sits in the noise floor. The mixing system is generated via source power spectral density models

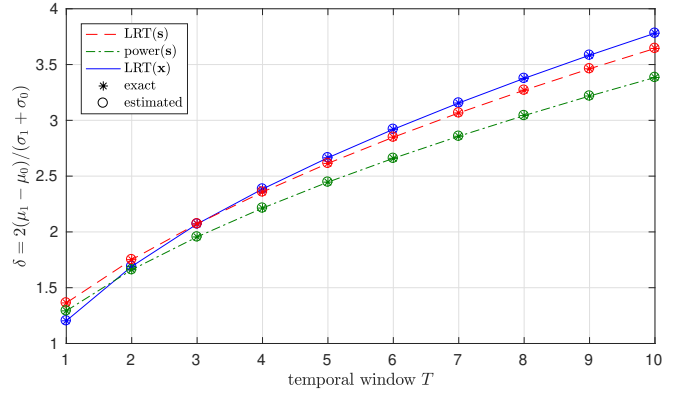


Fig. 2. Separability of distributions for setting with $J = 10$ and the transient source 10 dB below the stationary sources.

and a paraunitary mixing system, such that the ground truth space time covariance matrix $\mathbf{R}(z)$ is known for the LRT. It is also estimated from 10^5 snapshots of data using the best line unbiased estimator in [42] for GLRT results.

To compare the different methods, a good metric for the separation of distributions is the receiver operating characteristic (ROC) [68]. Here instead we work with scalar metric

$$\delta = \frac{|\mu_1 - \mu_0|}{(\sigma_0 + \sigma_1)/2}. \quad (31)$$

which define the separation distance between the distributions under hypotheses H_0 and H_1 . This metric δ assesses the ratio between the distributions' means μ_i , normalised by the mean of their standard deviations σ_i , for the two hypotheses H_i , $i = 0, 1$.

B. Simulations

For the setting with $J = 10$ and the transient signal sitting 10dB below the stationary signal in power, the results for the separability δ as defined in (31) is shown in Fig. 2 as a function of the temporal window T , $1 \leq T \leq 10$. For small values of T , decorrelating property of $\mathbf{Q}_\perp^P(z)$ give an advantage to the LRT operating on the projected data. Even just assessing the power of the projected data averaged over T snapshot without taking temporal correlation into account, as exploited in [11]–[13] and marked as power(s) in Fig. 2, provides an advantage over the LRT directly applied to the measurement data. Only as T is increased will the LRT of the measurement data outperform the other approaches, due to it additionally exploiting any information on the transient source that resides within the signal plus noise subspace.

Increasing the temporal correlation via $J = 20$ and now dropping the transient signal strength to match the noise floor, Fig. 3(a) show the separability. Now over the range of T , the LRT applied to the measurements is significantly worse compared to the LRT operating on the projected data. Also note that for $T > 8$, the GLRT results on the measurements dramatically deteriorate. When inspecting the involved matrices, it is not only that for e.g. $T = 10$, the LRT involves the inversion of 100×100 matrices for the measurement case

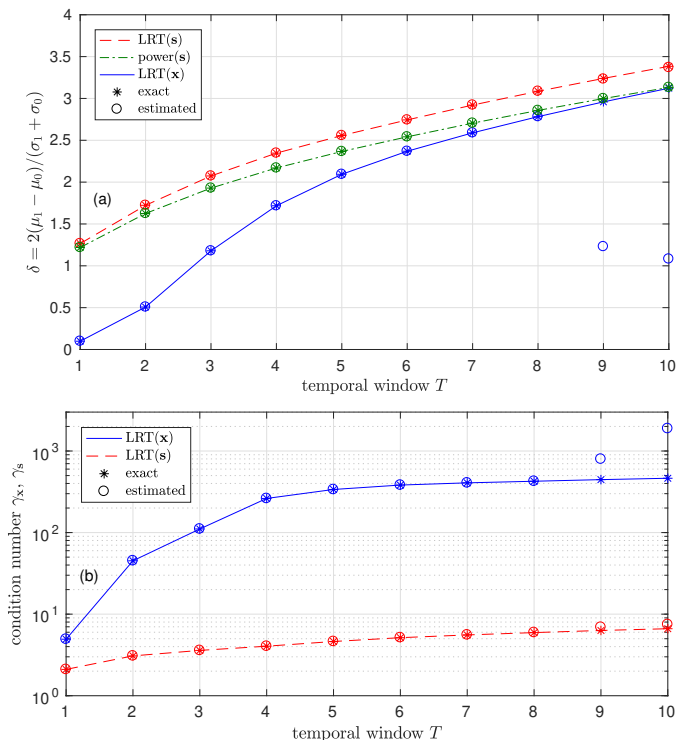


Fig. 3. (a) Separability of distributions and (b) condition numbers of covariance matrices for setting with $J = 20$ and the transient source 20 dB below the stationary sources.

as opposed to 30×30 matrices in the case of the projected data, but also that the condition numbers $\gamma_{x,1}$ and $\gamma_{s,1}$ as defined in Sec. IV-B significantly deviate. In case the condition numbers are determined for the estimated covariance matrices, for $T > 8$ deviations become noticeable in Fig. 3(b), which agrees with the performed drop for the measurement LRT in Fig. 3(a).

VI. DISCUSSION AND CONCLUSIONS

To detect a weak broadband transient signal, we have investigated the application of a likelihood ratio test to polynomial subspace-projected data rather than directly to the measurements. While for the stronger transient signals, the latter approach is optimal as it exploits all available information about the transient signal, the restriction to the noise-only subspace in the case of weaker transient signals had been shown to be beneficial. The subspace project approach ideally suppresses any strong stationary source components. This firstly removes any strong temporal correlations, which hinder the test, and secondly also significantly reduce the condition number of the covariance matrices that the LRT requires to be inverted, hence providing. As a result, the subspace-projected LRT operates on matrices that are decreased in both their dimension and condition number. This effect is the more pronounced the stronger the temporal correlations of the measured signals are and the weaker the transient signal is compared to the stationary sources.

REFERENCES

- [1] Z. Quan, S. Cui, H. V. Poor, and A. H. Sayed, "Collaborative wideband sensing for cognitive radios," *IEEE Signal Process. Mag.*, vol. 25, no. 6, pp. 60–73, Nov. 2008.
- [2] E. Axell, G. Leus, E. G. Larsson, and H. V. Poor, "Spectrum sensing for cognitive radio : State-of-the-art and recent advances," *IEEE Signal Process. Mag.*, vol. 29, no. 3, pp. 101–116, May 2012.
- [3] M. H. Al-Ali and K. C. Ho, "Objective Bayesian approach for binary hypothesis testing of multivariate Gaussian observations," *IEEE Trans. Information Theory*, vol. 69, no. 2, pp. 1337–1354, Feb. 2023.
- [4] A. Shukla, A. Alptekin, J. Bradford, E. Burbridge, D. Chandler, M. Kennett, P. Levine, and S. Weiss, "Cognitive radio technology — a study for ofcom," OFCOM, London, UK, Tech. Rep., Feb. 2007.
- [5] J. Renard, L. Lampe, and F. Horlin, "Sequential likelihood ratio test for cognitive radios," *IEEE Trans. Signal Process.*, vol. 64, no. 24, pp. 6627–6639, Dec. 2016.
- [6] J. Perez, J. Via, L. Vielva, and D. Ramirez, "Online detection and snr estimation in cooperative spectrum sensing," *IEEE Trans. Wireless Comms.*, vol. 21, no. 4, pp. 2521–2533, 2022.
- [7] C. A. D. Pahalon, L. H. Crockett, and S. Weiss, "Detection of weak transient broadband signals using a polynomial subspace and likelihood ratio test approach," in *European Signal Process. Conf.*, Lyon, France, pp. 1312–1316, Aug. 2024.
- [8] Z. Tong and X. Shuguo, "Design of a wideband signal detection circuit for electrical field sensor," in *Asia-Pacific Int. Symp. Electromagnetic Compatibility*, vol. 01, 2016, pp. 301–303.
- [9] R.-G. Ferber and H.-P. Harjes, "Adaptive processing of digital broadband seismic data," *IEEE Trans. Geoscience and Remote Sensing*, vol. 23, no. 6, pp. 789–796, 1985.
- [10] B. Yin, H. Shi, and Q. Liu, "A wideband transient signal detection method based on nonlinear support vector machine," in *4th Information Communication Technologies Conf.*, 2023, pp. 208–212.
- [11] S. Weiss, C. Delaosa, J. Matthews, I. Proudler, and B. Jackson, "Detection of weak transient signals using a broadband subspace approach," in *SSPD*, Edinburgh, Scotland, Sep. 2021, pp. 65–69.
- [12] V. W. Neo, S. Weiss, S. W. McKnight, A. O. T. Hogg, and P. A. Naylor, "Polynomial eigenvalue decomposition-based target speaker voice activity detection in the presence of competing talkers," in *IWAENC*, Bamberg, Germany, Sep. 2022.
- [13] V. W. Neo, S. Weiss, and P. A. Naylor, "A polynomial subspace projection approach for the detection of weak voice activity," in *SSPD*, London, UK, Sep. 2022, pp. 1–5.
- [14] B. Friedlander and B. Porat, "Detection of transient signals by the gabor representation," *IEEE Trans. Acoustics, Speech, and Signal Process.*, vol. 37, no. 2, pp. 169–180, Feb. 1989.
- [15] —, "Performance analysis of transient detectors based on a class of linear data transforms," *IEEE Trans. Information Theory*, vol. 38, no. 2, pp. 665–673, March 1992.
- [16] B. Porat and B. Friedlander, "Performance analysis of a class of transient detection algorithms—a unified framework," *IEEE Trans. Signal Process.*, vol. 40, no. 10, pp. 2536–2546, Oct. 1992.
- [17] S. Haykin, *Adaptive Filter Theory*, 2nd ed. Englewood Cliffs: Prentice Hall, 1991.
- [18] L. L. Scharf and B. Friedlander, "Matched subspace detectors," *IEEE Trans. Signal Process.*, vol. 42, no. 8, pp. 2146–2157, Aug 1994.
- [19] P. Strobach, "Low rank detection of multichannel gaussian signals using a constrained inverse," in *IEEE ICASSP*, vol. iv, Apr. 1994.
- [20] D. Lundstrom, M. Viberg, and A. M. Zoubir, "Multiple transient estimation using bootstrap and subspace methods," in *IEEE SSP*, Sep. 1998, pp. 184–187.
- [21] Zhen Wang and P. Willett, "A performance study of some transient detectors," *IEEE Trans. Signal Process.*, vol. 48, no. 9, pp. 2682–2685, Sep. 2000.
- [22] Zhen Wang and P. K. Willett, "All-purpose and plug-in power-law detectors for transient signals," *IEEE Trans. Signal Process.*, vol. 49, no. 11, pp. 2454–2466, Nov. 2001.
- [23] X. Li, Y. Wang, H. Ruan, B. Tang, and Y. Qin, "Deep manifold learning for weak signal detection," *IEEE Trans. Instrumentation and Measurement*, vol. 72, pp. 1–10, 2023.
- [24] O. Besson, "Maximum likelihood covariance matrix estimation from two possibly mismatched data sets," *Signal Process.*, vol. 167, p. 107285, Feb. 2020.

- [25] E. L. Lehmann and J. P. Romano, *Testing Statistical Hypotheses*, 4th ed. Springer, 2022.
- [26] A. Papoulis, *Probability, Random Variables, and Stochastic Processes*, 3rd ed. New York: McGraw-Hill, 1991.
- [27] P. P. Vaidyanathan, *Multirate Systems and Filter Banks*. Englewood Cliffs: Prentice Hall, 1993.
- [28] S. Weiss, J. Pestana, and I.K. Proudler, "On the existence and uniqueness of the eigenvalue decomposition of a parahermitian matrix," *IEEE Trans. Signal Process.*, vol. 66, no. 10, pp. 2659–2672, May 2018.
- [29] S. Weiss, J. Pestana, I.K. Proudler, and F.K. Coutts, "Corrections to 'On the existence and uniqueness of the eigenvalue decomposition of a parahermitian matrix'," *IEEE Trans. Signal Process.*, vol. 66, no. 23, pp. 6325–6327, Dec. 2018.
- [30] G. Barbarino and V. Noferini, "On the Rellich eigendecomposition of para-Hermitian matrices and the sign characteristics of $*$ -palindromic matrix polynomials," *Linear Algebra Appl.*, **672**:1–27, Sep. 2023.
- [31] S. Weiss, I.K. Proudler, G. Barbarino, J. Pestana, and J.G. McWhirter, "On properties and structure of the analytic singular value decomposition," *IEEE Trans. Signal Process.*, vol. 72, pp. 2260–2275, Apr. 2024.
- [32] S. Weiss, I. Proudler, F. Coutts, and F. Khattak, "Eigenvalue decomposition of a parahermitian matrix: extraction of analytic eigenvectors," *IEEE Trans. Signal Process.*, vol. 71, pp. 1642–1656, Apr. 2023.
- [33] J. Corr, K. Thompson, S. Weiss, I.K. Proudler, and J.G. McWhirter, "Row-shift corrected truncation of paraunitary matrices for PEVD algorithms," in *23rd European Signal Processing Conference*, Nice, France, pp. 849–853, Aug. 2015.
- [34] J. Corr, K. Thompson, S. Weiss, I.K. Proudler, and J.G. McWhirter, "Shortening of paraunitary matrices obtained by polynomial eigenvalue decomposition algorithms," in *Sensor Signal Processing for Defence*, Edinburgh, Scotland, Sep. 2015.
- [35] M. Tohidian, H. Amindavar, and A. M. Reza, "A DFT-based approximate eigenvalue and singular value decomposition of polynomial matrices," *J. Adv. Signal Process.*, vol. 2013, no. 1, pp. 1–16, 2013.
- [36] S. Weiss, I.K. Proudler, F.K. Coutts, and J. Pestana, "Iterative approximation of analytic eigenvalues of a parahermitian matrix EVD," in *IEEE Int. Conf. Acoustics, Speech and Signal Process.*, Brighton, UK, May 2019.
- [37] S. Weiss, I.K. Proudler, and F.K. Coutts, "Eigenvalue decomposition of a parahermitian matrix: extraction of analytic eigenvalues," *IEEE Trans. Signal Process.*, vol. 69, pp. 722–737, 2021.
- [38] S. Weiss, I.K. Proudler, F.K. Coutts, and J. Deeks, "Extraction of analytic eigenvectors from a parahermitian matrix," in *Int. Conf. Sensor Signal Processing or Defence*, Edinburgh, UK, 2020.
- [39] F.A. Khattak, I.K. Proudler, and S. Weiss, "Scalable extraction of analytic eigenvalues from a parahermitian matrix," in *32nd European Signal Processing Conf.*, Lyon, France, pp. 1317–1321, Aug. 2024.
- [40] F.A. Khattak, I.K. Proudler, and S. Weiss, "Scalable analytic eigenvalue extraction algorithm," *IEEE Access*, 2024, submitted.
- [41] C. Delaosa, F.K. Coutts, J. Pestana, and S. Weiss, "Impact of space-time covariance estimation errors on a parahermitian matrix EVD," in *10th IEEE Workshop on Sensor Array and Multichannel Signal Processing*, pp. 1–5, July 2018.
- [42] C. Delaosa, J. Pestana, N. J. Goddard, S. Somasundaram, and S. Weiss, "Sample space-time covariance matrix estimation," in *IEEE Int. Conf. Acoustics, Speech and Signal Processing*, Brighton, UK, May 2019, pp. 8033–8037.
- [43] F.A. Khattak, S. Weiss, I.K. Proudler, and J.G. McWhirter, "Space-time covariance matrix estimation: Loss of algebraic multiplicities of eigenvalues," in *56th Asilomar Conference on Signals, Systems, and Computers*, Pacific Grove, CA, Oct. 2022.
- [44] M. Bakhit, F.A. Khattak, I.K. Proudler, and S. Weiss, "Impact of estimation errors of a matrix of transfer functions onto its analytic singular values and their potential algorithmic extraction," in *IEEE High Performance Extreme Computing Conf.*, Boston, MA, Sep. 2024.
- [45] J.G. McWhirter, P.D. Baxter, T. Cooper, S. Redif, and J. Foster, "An EVD algorithm for para-Hermitian polynomial matrices," *IEEE Trans. Signal Process.*, vol. 55, no. 5, pp. 2158–2169, May 2007.
- [46] S. Redif, J.G. McWhirter, and S. Weiss, "Design of FIR paraunitary filter banks for subband coding using a polynomial eigenvalue decomposition," *IEEE Trans. Signal Process.*, **59**(11):5253–5264, Nov. 2011.
- [47] S. Redif, S. Weiss, and J.G. McWhirter, "An approximate polynomial matrix eigenvalue decomposition algorithm for para-hermitian matrices," in *11th IEEE Int. Symp. Signal Processing and Information Technology*, Bilbao, Spain, pp. 421–425, Dec. 2011.
- [48] S. Redif, S. Weiss, and J. McWhirter, "Sequential matrix diagonalization algorithms for polynomial EVD of parahermitian matrices," *IEEE Trans. Signal Process.*, vol. 63, no. 1, pp. 81–89, Jan. 2015.
- [49] J. Corr, K. Thompson, S. Weiss, J. McWhirter, S. Redif, and I. Proudler, "Multiple shift maximum element sequential matrix diagonalisation for parahermitian matrices," in *IEEE Workshop on Statistical Signal Processing*, Gold Coast, Australia, pp. 312–315, June 2014.
- [50] J. Corr, K. Thompson, S. Weiss, J. McWhirter, and I. Proudler, "Maximum energy sequential matrix diagonalisation for parahermitian matrices," in *48th Asilomar Conf. Signals, Systems and Computers*, Pacific Grove, CA, pp. 470–474, Nov. 2014.
- [51] Z. Wang, J.G. McWhirter, J. Corr, and S. Weiss, "Multiple shift second order sequential best rotation algorithm for polynomial matrix EVD," in *European Signal Process. Conf.*, Nice, France, pp. 844–848, Sep. 2015.
- [52] J.G. McWhirter and Z. Wang, "A novel insight to the SBR2 algorithm for diagonalising para-hermitian matrices," in *11th IMA Conf. on Mathematics in Signal Processing*, Birmingham, UK, Dec. 2016.
- [53] F.K. Coutts, I.K. Proudler, and S. Weiss, "Efficient implementation of iterative polynomial matrix evd algorithms exploiting structural redundancy and parallelisation," *IEEE Trans. Circuits and Systems I: Regular Papers*, vol. 66, no. 12, pp. 4753–4766, Dec. 2019.
- [54] F.A. Khattak, S. Weiss, and I.K. Proudler, "Fast givens rotation approach to second order sequential best rotation algorithms," in *Int. Conf. Sensor Signal Process. for Defence*, Edinburgh, UK, pp. 40–44, Sep. 2021.
- [55] J. Foster, J.G. McWhirter, and J.A. Chambers, "Limiting the order of polynomial matrices within the SBR2 algorithm," in *IMA Int. Conf. on Mathematics in Signal Processing*, Cirencester, UK, Dec. 2006.
- [56] C.H. Ta and S. Weiss, "Shortening the order of paraunitary matrices in SBR2 algorithm," in *6th Int. Conf. Information, Communications & Signal Processing*, Singapore, pp. 1–5, Dec. 2007.
- [57] F. Labeau, J.-C. Chiang, M. Kieffer, P. Duhamel, L. Vandendorpe, and B. Macq, "Oversampled filter banks as error correcting codes: theory and impulse noise correction," *IEEE Trans. Signal Process.*, vol. 53, no. 12, pp. 4619–4630, 2005.
- [58] S. Weiss, S. Redif, T. Cooper, C. Liu, P. Baxter, and J.G. McWhirter, "Paraunitary oversampled filter bank design for channel coding," *EURASIP J. Advances in Signal Processing*, vol. 2006, pp. 1–10, 2006.
- [59] M. Alrmah, S. Weiss, and S. Lambotharan, "An extension of the MUSIC algorithm to broadband scenarios using polynomial eigenvalue decomposition," in *19th European Signal Processing Conference*, Barcelona, Spain, pp. 629–633, Aug. 2011.
- [60] S. Weiss, M. Alrmah, S. Lambotharan, J.G. McWhirter, and M. Kaveh, "Broadband angle of arrival estimation methods in a polynomial matrix decomposition framework," in *IEEE 5th International Workshop on Computational Advances in Multi-Sensor Adaptive Processing*, St. Martin, pp. 109–112, Dec. 2013.
- [61] A. Hogg, V. Neo, S. Weiss, C. Evers, and P.A. Naylor, "A polynomial eigenvalue decomposition MUSIC approach for broadband sound source localization," in *IEEE Workshop on Applications of Signal Processing to Audio and Acoustics*, New Paltz, NY, Oct. 2021.
- [62] S. Redif, S. Weiss, and J.G. McWhirter, "Relevance of polynomial matrix decompositions to broadband blind signal separation," *Signal Process.*, vol. 134, pp. 76–86, May 2017.
- [63] V. Neo, C. Evers, S. Weiss, and P. Naylor, "Signal compaction using polynomial EVD for spherical array processing with applications," *IEEE/ACM Transactions on Audio, Speech, and Language Processing*, vol. 31, pp. 3537–3549, 2023.
- [64] S. Weiss, S. Bendoukha, A. Alzin, F. Coutts, I. Proudler, and J. Chambers, "MVDR broadband beamforming using polynomial matrix techniques," in *23rd European Signal Processing Conf.*, Nice, France, pp. 839–843, Sep. 2015.
- [65] V. Neo, S. Redif, J.G. McWhirter, J. Pestana, I.K. Proudler, S. Weiss, and P.A. Naylor, "Polynomial eigenvalue decomposition for multichannel broadband signal processing," *IEEE Signal Process. Mag.*, vol. 40, no. 7, pp. 18–37, Nov. 2023.
- [66] S. Weiss, N.J. Goddard, S. Somasundaram, I.K. Proudler, and P.A. Naylor, "Identification of broadband source-array responses from sensor second order statistics," in *Sensor Signal Processing for Defence Conf.*, London, UK, pp. 1–5, Dec. 2017.
- [67] G.H. Golub and C.F. Van Loan, *Matrix Computations*, 3rd ed. Baltimore, Maryland: John Hopkins University Press, 1996.
- [68] J.A. Hanley and B.J. McNeil, "The meaning and use of the area under a receiver operating characteristic (ROC) curve," *Radiology*, vol. 143, pp. 26–36, 1982.